

# PHOTOPRODUCTION OF $\omega$ AND $\omega$ IN THE NUCLEAR MEDIUM

*E. Oset<sup>a</sup>, M. Kaskulov<sup>b</sup>, H. Nagahiro<sup>c</sup>, E. Hernandez<sup>d</sup> and S. Hirenzaki<sup>e 1</sup>*

<sup>a</sup>Dpto. Física Teórica and IFIC<sup>2</sup>

<sup>b</sup>Institut für Physik, Giessen, Germany

<sup>c</sup>Research Center for Nuclear Physics, Osaka University, Ibaraki, Osaka

<sup>d</sup>Facultad de Ciencias, Universidad de Salamanca, Salamanca, Spain

<sup>e</sup>Department of Physics, Nara Women's University, Nara 630-8506 Japan

## Abstract

We reanalyze data from ELSA on  $\omega$  production in nuclei, from where claims of a large shift of the mass were made earlier, which are tied to a certain election of the background in nuclei, very different in shape to the one on the proton. The reanalysis shows that the data demand a very large width of the  $\omega$  in the medium, with no need for a shift of the mass, for which the experiment is quite insensitive. We study possible  $\omega$  bound states in the nucleus and find that, even assuming a small width, they could not be observed with the present ELSA resolution. Finally we show that, due to the interplay of background and  $\omega$  signal, a two bump structure appears with the ELSA set up for the  $(\gamma, p)$  reaction that should not be misidentified with a signal of a possible  $\omega$  bound state in the nucleus.

## 1 Introduction

The interaction of vector mesons with nuclei has captured for long the attention of the hadron community. Along these lines, an approach has been followed by the CBELSA/ TAPS collaboration by looking at the  $\gamma\pi^0$  coming from the  $\omega$  decay, where a recent work [1] claims evidence for a decrease of the  $\omega$  mass in the medium of the order of 100 MeV from the study of the modification of the mass spectra in  $\omega$  photoproduction. Here we present the reanalysis of the data of [1] done in [2], where one concludes that the distribution is compatible with an enlarged  $\omega$  width of about 90 MeV at

---

<sup>1</sup>IFIC, Universidad de Valencia, Spain.

<sup>2</sup>IFIC, Institutos de Investigacion, Universidad de Valencia, apdo 22085, 46071 Valencia, Spain.

nuclear matter density and no shift in the mass and at the same time we show the insensitivity of the results to a mass shift. We also show results for the  $(\gamma, p)$  reaction searching for possible  $\omega$  bound states in the nucleus concluding that even in the case of a sufficiently attractive potential and small width no peaks can be seen with the present experimental resolution of about  $50\text{MeV}$  at ELSA. We also discuss the origin of a two peak structure of the  $(\gamma, p)$  cross section which should not be misidentified with evidence for an  $\omega$  bound state in the nucleus.

## 2 Preliminaries

We consider the photonuclear reaction  $A(\gamma, \omega \rightarrow \pi^0\gamma)X$  in two steps - production of the  $\omega$ -mesons and propagation of the final states. In the laboratory, where the nucleus with the mass number  $A$  is at rest, the nuclear total cross section of the inclusive reaction  $A(\gamma, \omega)X$ , including the effects of Fermi motion and Pauli blocking, plus effects of final state interaction of the particles produced, can be calculated as shown in [2].

The  $\omega$ -mesons are produced according to their spectral function  $S_\omega$  at a local density  $\rho(r)$

$$S_\omega(m_\omega, \tilde{m}_\omega, \rho) = -\frac{1}{\pi} \frac{\text{Im}\Pi_\omega(\rho)}{\left(\tilde{m}_\omega^2 - m_\omega^2 - \text{Re}\Pi_\omega(\rho)\right)^2 + \left(\text{Im}\Pi_\omega(\rho)\right)^2}, \quad (1)$$

where  $\Pi_\omega$  is the in-medium selfenergy of the  $\omega$ . The width of the  $\omega$  in the nuclear medium is related to the selfenergy by  $\Gamma_\omega(\rho, \tilde{m}_\omega) = -\text{Im}\Pi_\omega(\rho, \tilde{m}_\omega)/E_\omega$ . It includes the free width  $\Gamma_{free} = 8.49$  MeV and an in-medium part  $\Gamma_{coll}(\rho)$  which accounts for the collisional broadening of the  $\omega$  due to the quasielastic and absorption channels. In Eq. (1)  $\text{Re}\Pi_\omega = 2E_\omega\text{Re}V_{opt}(\rho)$ , where  $V_{opt}(\rho)$  is the  $\omega$  nucleus optical potential accounts for a possible shift of the  $\omega$  mass in the medium and we shall make some considerations about it latter on.

We also consider the situation when the energy of the incident photon beam is not fixed but constrained in some energy interval  $E_\gamma^{\min} < E_\gamma < E_\gamma^{\max}$ , and also take into account the photon flux produced at the ELSA facility.

## 3 The Monte Carlo simulation procedure

The computer MC simulation proceeds in close analogy to the actual experiment. At first, the multiple integral involved in the evaluation of the cross

section is carried out using the MC integration method. This procedure provides a random point  $\vec{r}$  inside the nucleus where the photon collides with the nucleon, also randomly generated from the Fermi sea with  $|\vec{p}_N| \leq k_F(\vec{r})$ . For the sample event in the MC integral the mass  $\tilde{m}_\omega$  of the  $\omega$  respects the spectral function  $S_\omega$  at local density  $\rho(r)$ , see Eq. (1). Inside the nucleus the  $\omega$ -mesons moving with the three momentum  $\vec{p}_\omega^{lab}$  necessarily interact with the nucleons in their way out of the nucleus. In the MC simulation the  $\omega$ -mesons are allowed to propagate a distance  $\delta\vec{L} = \frac{\vec{p}_\omega^{lab}}{|\vec{p}_\omega^{lab}|} \delta L$  and at each step,  $\delta L \simeq 0.1$  fm, the reaction probabilities for different channels like the decay of the  $\omega$  into  $\pi^0\gamma$  and  $\pi\pi\pi$  final states, quasielastic scattering and in-medium absorption are properly calculated. Details of the simulation can be seen in [2].

We use the following parameterization for the width,  $\Gamma_{abs} = \Gamma_0 \frac{\rho(r)}{\rho_0}$ , where  $\rho_0 = 0.16$  fm $^{-3}$  is the normal nuclear matter density.

The propagation of pions in nuclei is done using a MonteCarlo simulation procedure. In their way out of the nucleus pions can experience the quasielastic scattering or can be absorbed. The intrinsic probabilities for these reactions as a function of the nuclear matter density are calculated using the phenomenological model of Refs [3], which also includes higher order quasielastic cuts and the two-body and three-body absorption mechanisms. Details for the present case are described in [2].

## 4 In-medium $\omega$ -meson width and nuclear transparency

In this section we discuss an extraction of the in-medium inelastic width of the  $\omega$  in the photonuclear experiments. As a measure for the  $\omega$ -meson width in nuclei we employ the so-called nuclear transparency ratio

$$\tilde{T}_A = \frac{\sigma_{\gamma A \rightarrow \omega X}}{A \sigma_{\gamma N \rightarrow \omega X}} \quad (2)$$

i.e. the ratio of the nuclear  $\omega$ -photoproduction cross section divided by  $A$  times the same quantity on a free nucleon.  $\tilde{T}_A$  describes the loss of flux of  $\omega$ -mesons in the nuclei and is related to the absorptive part of the  $\omega$ -nucleus optical potential and thus to the  $\omega$  width in the nuclear medium.

We have done the MC calculations for the sample nuclear targets:  ${}^{12}_6\text{C}$ ,  ${}^{16}_8\text{O}$ ,  ${}^{24}_{12}\text{Mg}$ ,  ${}^{27}_{13}\text{Al}$ ,  ${}^{28}_{14}\text{Si}$ ,  ${}^{31}_{15}\text{P}$ ,  ${}^{32}_{16}\text{S}$ ,  ${}^{40}_{20}\text{Ca}$ ,  ${}^{56}_{26}\text{Fe}$ ,  ${}^{64}_{29}\text{Cu}$ ,  ${}^{89}_{39}\text{Y}$ ,  ${}^{110}_{48}\text{Cd}$ ,  ${}^{152}_{62}\text{Sm}$ ,  ${}^{208}_{82}\text{Pb}$ ,  ${}^{238}_{92}\text{U}$ . In the following we evaluate the ratio between the nuclear cross sections in heavy nuclei and a light one, for instance  ${}^{12}\text{C}$ , since in this way, many other nuclear effects not related to the absorption of the  $\omega$  cancel in the ratio,  $T_A$ .

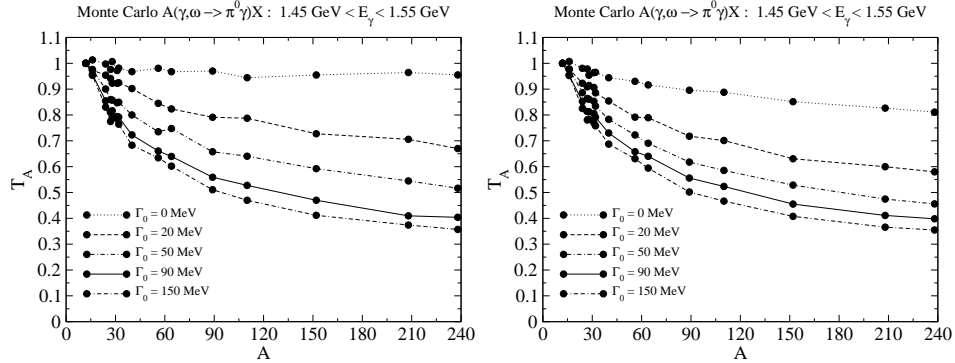


Figure 1: The result of the Monte Carlo method for the  $A$ -dependence of the nuclear transparency ratio  $T_A$  without (left panel) and with (right panel) FSI of outgoing pions. A lower cut  $T_\pi > 150$  MeV on the kinetic energy of the outgoing pions has been used to suppress the contribution of the distorted events due to FSI. The incident photon beam was constrained in the range  $1.45 \text{ GeV} < E_\gamma < 1.55 \text{ GeV}$ . The carbon  $^{12}\text{C}$  was used as the reference target in the ratio of the nuclear cross sections. With  $\Gamma_{abs} = \Gamma_0 \frac{\rho(r)}{\rho_0}$ , where  $\rho_0$  is the normal nuclear matter density, the dotted, dashed, dash-dotted, solid and dash-dash-dotted curves correspond to  $\Gamma_0 = 0 \text{ MeV}$ ,  $\Gamma_0 = 20 \text{ MeV}$ ,  $\Gamma_0 = 50 \text{ MeV}$ ,  $\Gamma_0 = 90 \text{ MeV}$  and  $\Gamma_0 = 150 \text{ MeV}$ , respectively.

The results of the MC calculation for the  $A$ -dependence of the nuclear transparency ratio  $T_A$  are presented in Fig. 1. The incident photon beam was constrained in the range  $1.45 \text{ GeV} < E_\gamma < 1.55 \text{ GeV}$  - a region which is considered in the analysis of the CBELSA/TAPS experiment [4, 5]. In Fig. 1 (left panel) we show the results for the transparency ratio when the collisional broadening and FSI of the  $\omega$  are taken into account but without FSI of the pions from  $\omega \rightarrow \pi^0\gamma$  decays inside the nucleus. The right panel corresponds to considering in addition the FSI of the pions.

By using these results and taking into account the preliminary results of CBELSA/TAPS experiment [5] we get an estimate for the  $\omega$  width  $\Gamma_{abs} \simeq 90 \times \frac{\rho(r)}{\rho_0} \text{ MeV}$ . This estimate must be understood as an average over the  $\omega$  three momentum.

## 5 In-medium $\omega$ -meson mass and CBELSA/TAPS experiment

The first thing one should note is that the  $\omega$  line shape reconstructed from  $\pi^0\gamma$  events strongly depends on the background shape subtracted from the bare  $\pi^0\gamma$  signal. In Ref. [1] the shape of the background was chosen such that

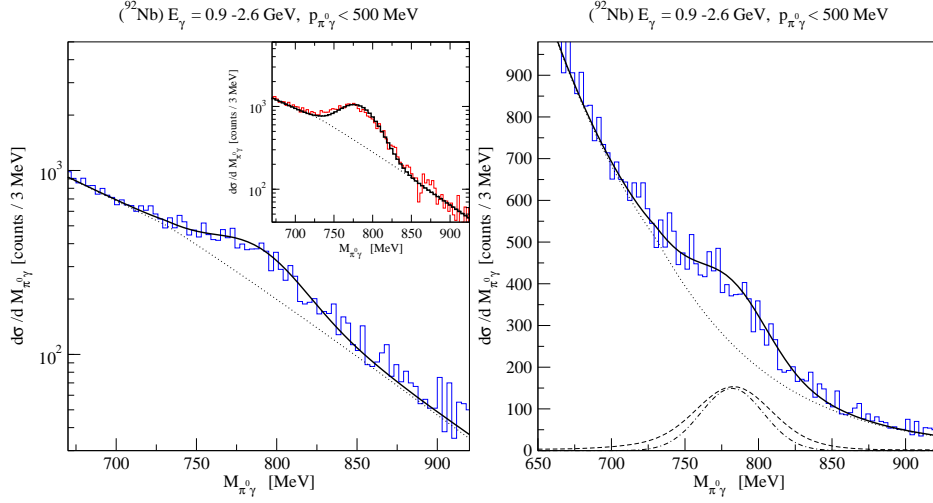


Figure 2: Left panel: Invariant mass spectra reconstructed from the  $\pi^0\gamma$  events in the  $(\gamma, \pi^0\gamma)$  reaction from Nb target (solid curve). The experimental data are from Ref. [1]. The incident photon beam has been constrained in the range  $0.9 \text{ GeV} < E_\gamma^{in} < 2.6 \text{ GeV}$ . Dotted curve is an uncorrelated  $\pi^0\gamma$  background (see the text). Right panel: Same but in linear scale. The dashed and dash-dash-dotted curves correspond to the  $\omega \rightarrow \pi^0\gamma$  events with and without the kinematic cut  $|\vec{p}_{\pi^0\gamma}| < 500 \text{ MeV}$ , respectively. The normalization without cut is arbitrary. The solid line corresponds to the sum of the background and the dashed line. Inset (left panel): The  $\pi^0\gamma$  invariant mass spectra in the elementary  $p(\gamma, \pi^0\gamma)p$  reaction. Same background line shape (dotted curve) as for the Nb target has been used. The solid line is the sum of the background and  $\omega \rightarrow \pi^0\gamma$  events.

it accounted for all the experimental strength at large invariant masses. This choice was done both for the elementary  $\gamma p \rightarrow \pi^0\gamma p$  reaction as well as for nuclei. As we shall show, this choice of background in nuclei implies a change of the shape from the elementary reaction to that in the nucleus for which no justification was given. We shall also show that when the same shape for the background as for the elementary reaction is chosen, the experiment in nuclei shows strength at invariant masses higher than  $m_\omega$  where the choice of [1] necessarily produced no strength. We will also see that the experimental data can be naturally interpreted in terms of the large in-medium  $\omega$  width discussed above without the need to invoke a shift in the  $\omega$  mass in the medium.

In Fig. 2 we show the experimental data (solid histogram) for the  $\pi^0\gamma$  invariant mass spectra in the reaction  $(\gamma, \pi^0\gamma)$  [1] from  $^{92}_{41}\text{Nb}$  target. The inset (left panel) corresponds to the  $\pi^0\gamma$  spectra from the hydrogen target. In our MC calculations the incident photon beam has been constrained in the range  $0.9 \text{ GeV} < E_\gamma^{in} < 2.6 \text{ GeV}$ . The higher momentum cut  $|\vec{p}_{\pi^0\gamma}| =$

$|\vec{p}_{\pi^0} + \vec{p}_\gamma| < 500$  MeV on a three momentum of the  $\pi^0\gamma$  pair was imposed as in the actual experiment. First, we use the hydrogen target, see inset in Fig. 2 (left panel), to fix the contribution of the uncorrelated  $\pi^0\gamma$  background (dotted curve) which together with the  $\pi^0\gamma$  signal from  $\omega \rightarrow \pi^0\gamma$  decay, folded with the Gaussian experimental resolution of 55 MeV as in Ref. [1], gives a fair reproduction of the experimental spectra. Then we assume the same shape of the  $\pi^0\gamma$  background in the photonuclear reaction. The weak effect of the FSI of the pions found in the calculation, with the cuts imposed in the experiment, strongly supports this assumption.

In the following we use the  $\omega$  inelastic width of  $\Gamma_0 = 90$  MeV at  $\rho_0$ . The exclusive  $\omega \rightarrow \pi^0\gamma$  MC spectra is shown by the dashed curve (right panel). The solid curve is the reconstructed  $\pi^0\gamma$  signal after applying the cut on  $\pi^0\gamma$  momenta and adding the background fixed when using the hydrogen target (dotted curve). Note that the shape of the exclusive  $\pi^0\gamma$  signal without applying a cut on  $\pi^0\gamma$  momenta (dash-dotted curve) is dominated by the experimental resolution and no broadening of the  $\omega$  is observed. This is in agreement with data of Ref. [1]. But applying the cut one increases the fraction of in-medium decays coming from the interior of the nucleus where the spectral function is rather broad and as a result the broadening of the  $\pi^0\gamma$  signal with respect to the signal (without cut) can be well seen. The resulting MC spectra (solid curve) shows the accumulation of the  $\pi^0\gamma$  events from the left and right sides of the mass spectra, and it is consistent both with our choice of the uncorrelated  $\pi^0\gamma$  background and experimental data.

We have also done the exercise of seeing the sensitivity of the results to changes in the mass. As shown in [2], a band corresponding to having the  $\omega$  mass in between  $m_\omega \pm 40\rho/\rho_0$  MeV is far narrower than the statistical fluctuations. In other words, this experiment is too insensitive to changes in the mass to be used for a precise determination of the shift of the  $\omega$ -mass in the nuclear medium. We should also note that the peak position barely moves since it is dominated by the decay of the  $\omega$  outside the nucleus.

## 6 Production of bound $\omega$ states in the $(\gamma,p)$ reaction

Here we evaluate the formation rate of  $\omega$  bound states in the nucleus by means of the  $(\gamma,p)$  reaction. We use the Green function method [6] to calculate the cross sections for  $\omega$ -mesic states formation as described in Refs. [7] in detail. The theoretical model used here is exactly same as that used in these references.

The  $\omega$ -nucleus optical potential is written here as  $V(r) = (V_0 + iW_0)\frac{\rho(r)}{\rho_0}$ , where  $\rho(r)$  is the nuclear experimental density for which we take the two parameter Fermi distribution. We consider three cases of the potential strength as:  $(V_0, W_0) = -(0, 50)$ ,  $-(100, 50)MeV$  and  $-(156, 29)MeV$ . The last of the potentials is obtained by the linear density approximation with the scattering length  $a = 1.6 + 0.3i$  fm [8]. This potential is strongly attractive with weak absorption and hence should be the ideal case for the formation of  $\omega$  mesic nuclei. No  $\omega$  bound states are expected for the first potential which has only an absorptive part. The second potential has a strong attraction with the large absorptive part as indicated in Ref. [4]. For the first two potentials we find no visible peaks in the spectrum since the width is so large. For the third potential we observe peaks but they are washed out when folded with the experimental resolution of about  $50MeV$  of ELSA.

## 7 Monte Carlo simulation of the reaction of the $(\gamma, p)$ reaction

We next apply the MonteCarlo simulation explained above to describe the  $(\gamma, p)$  reaction studied at ELSA. Because our MC calculations represent complete event simulations it is possible to take into account the actual experimental acceptance of ELSA [4] (see details in [9]).

We start our MC analysis with the cross section of the elementary reaction  $\gamma p \rightarrow \omega p \rightarrow \pi^0 \gamma p$ . With this we determine the cross section for  $\omega$  formation and follow the fate of the protons at the same time.

There are also sources of background like from  $\gamma p \rightarrow \pi^0 \pi^0 p$ , or  $\gamma p \rightarrow \pi^0 \eta p$ , where one of the two photons from the decay of the  $\pi^0$  or the  $\eta$  is not measured. We show in Fig. 3 the cross section  $d\sigma/dE_{\pi^0 \gamma}$  coming from the  $\gamma p \rightarrow \pi^0 \pi^0 p$  reaction followed by the decay  $\pi^0 \rightarrow \gamma \gamma$  of either of the  $\pi^0$  (left panel) and from the  $\gamma p \rightarrow \pi^0 \eta p$  reaction followed by the decay  $\eta \rightarrow \gamma \gamma$  (right panel). As one can see, the contribution from the  $\pi^0 \pi^0$  photoproduction to the background is the dominant one among the two. The important thing, thus, is that these two sources of background, with the cuts imposed, produce a background peaked at -100 MeV. For the exclusive  $\pi^0 \gamma$  events coming from  $\gamma p \rightarrow \omega p \rightarrow \pi^0 \gamma p$  an experimental resolution of 50 MeV was imposed, see Ref. [1]. We obtain a factor of two bigger strength at the  $\omega$  peak than at the peak from the  $\gamma p \rightarrow \pi^0 \pi^0 p$  background. Experimentally, this seems to be also the case from the preliminary data of CBELSA/TAPS,

In the following we assume that the inclusive  $\pi^0 \gamma$  background scales with respect to the target nucleus mass number  $A$  like  $\sigma_A \simeq A \sigma_{elem}$ . But this

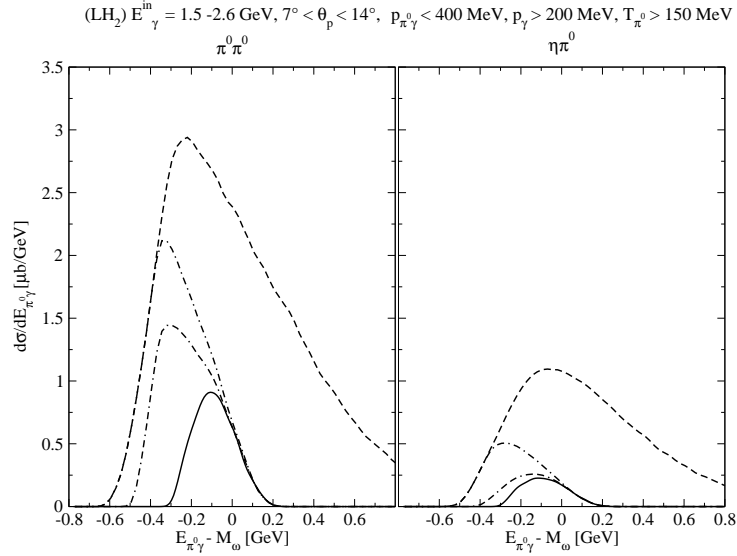


Figure 3: The differential cross section  $d\sigma/dE_{\pi^0\gamma}$  of the reactions  $\gamma p \rightarrow \pi^0\pi^0 p$  (left panel) and  $\gamma p \rightarrow \pi^0\eta p$  (right panel) followed by the decay  $\pi^0(\eta) \rightarrow \gamma\gamma$  as a function of the  $E_{\pi^0\gamma} - m_\omega$  where  $E_{\pi^0\gamma} = E_{\pi^0} + E_\gamma$ . The following cuts were imposed:  $E_\gamma^{in} = 1.5 \div 2.6$  GeV and  $7^\circ < \theta_p < 14^\circ$  (dashed curves);  $E_\gamma^{in} = 1.5 \div 2.6$  GeV,  $7^\circ < \theta_p < 14^\circ$  and  $|\vec{p}_{\pi^0} + \vec{p}_\gamma| < 400$  MeV (dash-dotted curves); plus the cut  $T_{\pi^0} > 150$  MeV (dash-dash-dotted curves) and plus the cut  $|\vec{p}_\gamma| > 200$  MeV (solid curves).

is not the case for the exclusive  $\pi^0\gamma$  events coming from the decay of the  $\omega \rightarrow \pi^0\gamma$ , since the rather strong absorption of the  $\omega$  inside the nucleus changes the scaling relation and  $\sigma_A(\omega \rightarrow \pi^0\gamma) \simeq A^\alpha \sigma_{elem}(\omega \rightarrow \pi^0\gamma)$ , where the attenuation parameter  $\alpha < 1$ .

In Fig. 4 we show the result of the MC simulation for the  $E_{\pi^0\gamma} - m_\omega$  spectra reconstructed from the  $\pi^0$  and  $\gamma$  events. The calculations are performed for the sample nuclear targets  $^{12}\text{C}$ ,  $^{40}\text{Ca}$ ,  $^{92}\text{Nb}$  and  $^{208}\text{Pb}$ . The kinematic and acceptance cuts discussed before have been already imposed. The MC distributions are normalized to the nuclear mass number  $A$ . The solid curves correspond to the sum of the inclusive  $\pi^0\gamma$  background (dash-dotted curve), and the exclusive  $\pi^0\gamma$  events coming from the direct decay of the  $\omega \rightarrow \pi^0\gamma$ . The contributions of the exclusive  $\omega \rightarrow \pi^0\gamma$  events are shown by the dashed curves. We note a very strong attenuation of the  $\omega \rightarrow \pi^0\gamma$  signal with respect to the background contribution with increasing nuclear mass number  $A$ . This is primary due to the stronger absorption of the  $\omega$ -mesons with increasing nuclear matter density. The former exercise indicates that given the

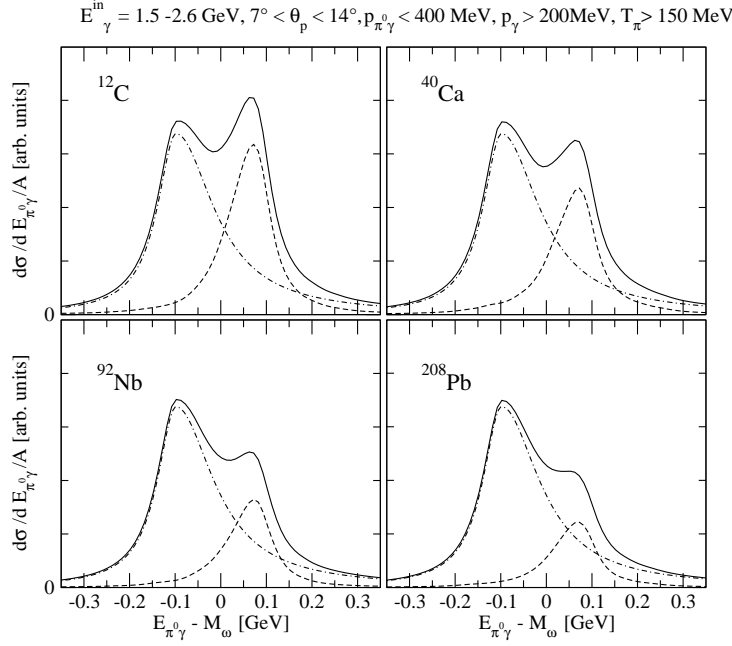


Figure 4: The differential cross section  $d\sigma/dE_{\pi^0\gamma}$  of the reaction  $A(\gamma, \pi^0\gamma)X$  as a function of  $E_{\pi^0\gamma} - m_{\omega}$  from  $^{12}\text{C}$ ,  $^{40}\text{Ca}$ ,  $^{92}\text{Nb}$  and  $^{208}\text{Pb}$  nuclear targets. The reconstructed exclusive events from the  $\omega \rightarrow \pi^0\gamma$  decay are shown by the dashed curves. The  $\pi^0\gamma$  background is shown by the dash-dotted curves. The sum of the two contributions is given by the solid curves. The following cuts were imposed:  $E_{\gamma}^{\text{in}} = 1.5 \div 2.6 \text{ GeV}$ ,  $7^{\circ} < \theta_p < 14^{\circ}$ ,  $|\vec{p}_{\pi^0} + \vec{p}_{\gamma}| < 400 \text{ MeV}$ ,  $|\vec{p}_{\gamma}| > 200 \text{ MeV}$  and  $T_{\pi} > 150 \text{ MeV}$ . The exclusive  $\omega \rightarrow \pi^0\gamma$  signal has been folded with the 50 MeV experimental resolution. All spectra are normalized to the corresponding nuclear mass numbers  $A$ .

particular combination of  $\pi^0\gamma$  from an uncorrelated background and from  $\omega$  decay, and the different behaviour of these two sources in the  $\pi^0\gamma$  production in nuclei, a double hump structure is unavoidable in nuclei with this set up, and one should avoid any temptation to associate the lower energy peak to a possible bound state in the nucleus.

## 8 Conclusions

The studies done in [2] and [9] show that: 1) The ELSA results on inclusive  $\omega$  production in nuclei can be interpreted in terms of a large  $\omega$  width in the medium without the need of a mass shift. 2) The results are very insensitive to a mass shift in matter. 3) With the large medium  $\omega$  width

derived from the ELSA data no visible peaks for  $\omega$  bound states are seen, even with hypothetical large  $\omega$  binding. 4) Even in the hypothetical case of small widths, the possible  $\omega$  bound states would not be resolved with the present ELSA resolution. 5) When looking at the  $(\gamma, p)$  reaction with the present ELSA experimental set up, a double hump structure appears in the calculation from the interplay of the  $\omega$  signal and the background. The peak at lower energies is related to the background, with the cuts imposed, and should not be misidentified with a possible  $\omega$  bound state in the nucleus.

## Acknowledgments

This work is partly supported by DGICYT contract number BFM2003-00856, the Generalitat Valenciana, the projects FPA2004-05616 (DGICYT) and SA016A07 (Junta de Castilla y Leon). This research is part of the EU Integrated Infrastructure Initiative Hadron Physics Project under contract number RII3-CT-2004-506078.

## 9 References

### References

- [1] D. Trnka *et al.* [CBELSA/TAPS Collaboration], Phys. Rev. Lett. **94** (2005) 192303
- [2] M. Kaskulov, E. Hernandez and E. Oset, Eur. Phys. J. A **31** (2007) 245
- [3] L. L. Salcedo, E. Oset, M. J. Vicente-Vacas and C. Garcia-Recio, Nucl. Phys. A **484** (1988) 557.
- [4] D. Trnka, PhD Thesis, University of Giessen, 2006.
- [5] M. Kotulla, [arXiv:nucl-ex/0609012].
- [6] O. Morimatsu, K. Yazaki, Nucl. Phys. A 435 (1985) 727;
- [7] D. Jido, H. Nagahiro, S. Hirenzaki, Phys. Rev. C 66 (2002) 045202;
- [8] F. Klingl, T. Waas and W. Weise, Nucl. Phys. A **650** (1999) 299
- [9] M. Kaskulov, H. Nagahiro, S. Hirenzaki and E. Oset, Phys. Rev. C 75 (2007) 064616

## **Author Index**

## Subject Index